ACS ES&T Water

pubs.acs.org/estwater

Article

Enhanced Adsorption of Mixtures of Per- and Polyfluoroalkyl Substances in Water by Chemically Modified Activated Carbon

Aswin Kumar Ilango,[‖] Tao Jiang,[‖] Weilan Zhang,* Md. Nahid Pervez, Jeremy I. Feldblyum, Haralabos Efstathiadis, and Yanna Liang

Cite This: *ACS EST Water* 2023, 3, 3708–3715

Read Online

ACCESS | Metrics & More | Article Recommendations | Supporting Information

ABSTRACT: Chemical modifications of granular activated carbon (GAC) and powdered activated carbon (PAC) are necessary for enhanced removal of perfluoroalkyl and polyfluoroalkyl substances (PFAS) in water. Herein, we synthesized and tested goethite (α-FeOOH)-coated GAC and PAC for the adsorption of mixtures of 13 PFAS (9 short- and long-chain PFAAs, GenX, and 3 precursors) from water at an initial concentration of 10 μg/L for each. Among the sorbents tested, modified PAC (MPAC) had excellent adsorption compared to pristine PAC and GAC and modified GAC (MGAC). Based on the isotherms, the maximum adsorption capacity of MPAC toward total PFAS removal was 234 mg/g. Detailed characterizations revealed that the adsorption performance of MPAC was due to its powdered nature, which enabled a shorter diffusion path and rapid mass transfer in the internal pores of this sorbent in addition to the electrostatic and hydrophobic interactions. Results obtained from this study provide valuable insights and knowledge for properly modifying GAC and PAC to address the critical challenges associated with PFAS, especially those associated with short-chain compounds.

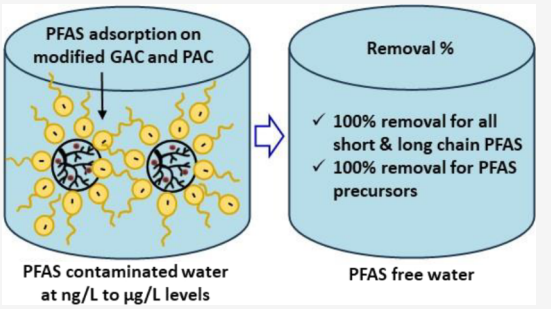

KEYWORDS: *modifications of GAC and PAC, PFAS adsorption, isotherm and kinetic studies, removal mechanism*

1. INTRODUCTION

Per- and polyfluoroalkyl substances (PFAS) are a class of synthetic chemicals characterized by a hydrophobic tail and a hydrophilic head. The hydrophilic head consists of polar functional groups such as carboxylate (COO^-), sulfonate (SO_3^-), and sulfonamides (SO_2N).[1,2] Because of their unique attributes, such as being resistant to degradation, persistent in the environment, and potentially harmful to ecosystems, PFAS pose a substantial threat to both environmental safety and human health.[3−5] In June 2022, the U.S. Environmental Protection Agency (EPA) issued the interim lifetime health advisory levels for perfluorooctanoic acid (PFOA) and perfluorooctanesulfonic acid (PFOS) in drinking water, which were set at extremely low concentrations of 0.004 and 0.02 ng/L, respectively.[6] The regulatory demand of these exceptionally low levels, combined with the stable C−F bonds within their structures, bring a major challenge for remediation efforts. As a result, novel and sustainable technologies are urgently needed to remove PFAS in water to such low concentrations.[7]

Conventional treatment methods have demonstrated their inefficacy in effectively eliminating PFAS.[8] For instance, biological treatment primarily focuses on breaking the C−C bond of PFAS, resulting in the rapid formation of short-chain PFAS in water.[9] Similarly, oxidation only partially degrades PFAS, resulting in the formation of PFAS molecules with shorter perfluorinated alkyl chains.[10] Chlorine or UV disinfection techniques are also futile in removing PFAS under typical water treatment conditions.[11,12] In contrast, adsorption has emerged as a well-established and reliable technology for PFAS removal, both as a standalone process for point-of-use applications and as a component of water treatment processes.[13,14]

Currently, a variety of commercial and synthetic sorbents have been documented in the literature for PFAS removal, including clays,[15] granular activated carbon (GAC),[16] powdered activated carbon (PAC),[17] resins,[18] and surface-modified biopolymers.[19] GAC and PAC have exhibited effectiveness in adsorbing long-chain PFAS, but both suffer from certain limitations. GAC, for instance, is well-known for its slow adsorption kinetics and comparatively lower efficiency in removing short-chain PFAS and precursors in comparison to long-chain counterparts.[20,21] On the other hand, superfine PAC facilitates the rapid diffusion of short-chain PFAS molecules for swift adsorption,[22] but its use leads to the formation of stable colloids in water, rendering their removal challenging and necessitating additional centrifugation or

Received: August 17, 2023
Revised: September 27, 2023
Accepted: September 28, 2023
Published: October 12, 2023

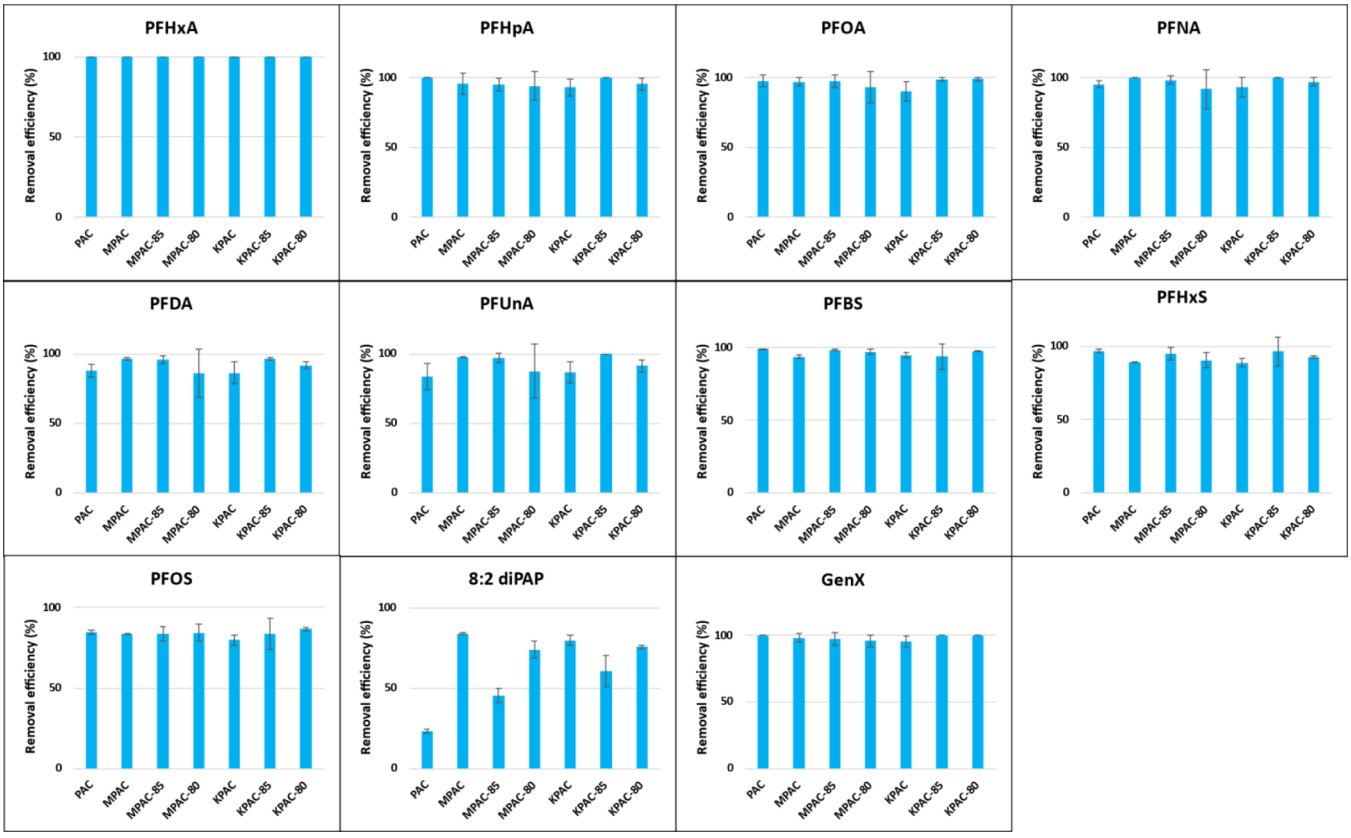

Figure 1. PFAS removal was by PAC and modified PAC at 48 h. Initial PFAS concentration: 100 ng/L, and sorbent dosage: 100 mg/L.

filtration steps. This drawback hampers the practical application of PAC in real-world drinking water treatment.[23] Consequently, to enhance the adsorption capabilities for the adsorption of short-chain PFAS and precursors, the modifications of both GAC and PAC are necessary.

Given that goethite (α-FeOOH), an abundant iron oxyhydroxide naturally found in sediments and rocks, is highly thermodynamically stable in nature,[24] α-FeOOH-based composites have been used for removing toxic anions from water. A precipitation method[25] was employed to coat iron oxide hydroxides (FeOOH) onto both GAC and PAC, resulting in modified GAC (MGAC) and modified PAC (MPAC). Although neither MGAC nor MPAC possesses magnetic properties, it was believed that the modification enhanced the electrostatic interactions[26] between PFAS (especially short-chain) and Fe^{3+} from both MGAC and MPAC.

Despite a few studies reporting the use of modified GAC and PAC for PFAS removal from water, most of them have focused solely on removing PFOA or PFOS at mg/L levels.[27] Therefore, it remains uncertain whether these sorbents can effectively remove PFAS mixtures comprising these compounds with diverse functional groups, structures (varying chain lengths), and concentrations as low as μg/L or ng/L. Hence, in this study, we synthesized FeOOH-assisted GAC and PAC composites with the expectation that they would exhibit a high adsorption capacity toward PFAS mixtures and display fast adsorption kinetics, particularly for short-chain PFAS. The results obtained from this study will provide valuable insights and knowledge for properly modifying GAC and PAC to address the critical challenges associated with PFAS, especially short-chain compounds.

2. EXPERIMENTAL SECTION

2.1. Materials and Preparation of MGAC and MPAC. The physiochemical properties of the 13 PFAS studied are listed in Table S1. The chemicals and reagents used in this study are listed in Table S2. Milli-Q water (resistivity ≥18.2 MΩ·cm) was used to prepare PFAS solutions. The synthesis procedure was developed from a method reported by Lee et al. with slight modifications.[25] Briefly, PAC was first added to a 65 g/L NH_4HCO_3 solution. Then, $FeCl_3$ solution at 35 wt % was titrated slowly into the mixture of NH_4HCO_3 and PAC solution at a mass ratio of $FeCl_3$:NH_4HCO_3 = 1:5.5. The mass ratio of PAC to α-FeOOH was 90:10, 85:15, or 80:20. During the reactions, the pH was set at 7.0. After agitating continuously for 2 h, the mixture was centrifuged at 3500 rpm for 15 min. The supernatant was discarded, and the solid product was washed with deionized water three times. The washed sorbent was then freeze-dried overnight. The same procedure was also used to prepare MPAC with α-FeOOH and kaolin at different ratios, as shown in Table S3. As shown below, because MPAC 90:10 had the best adsorption performance, MGAC with GAC:α-FeOOH at 90:10 was also prepared in a similar fashion.

2.2. PFAS Adsorption Experiments. Adsorption experiments were performed in batch mode and in triplicate. To investigate the improvement of PFAS adsorption on PAC by surface modification, each FeOOH- or FeOOH- and kaolin-modified sorbent (Table S3) was added at 100 mg/L to a PFAS solution consisting of six PFCAs (C6−C11), three PFSAs (C4, C6, and C8), 8:2 diPAP, and GenX, with each at 100 ng/L. The mixture was then kept on a rotating shaker at

https://doi.org/10.1021/acsestwater.3c00483
ACS EST Water 2023, 3, 3708−3715

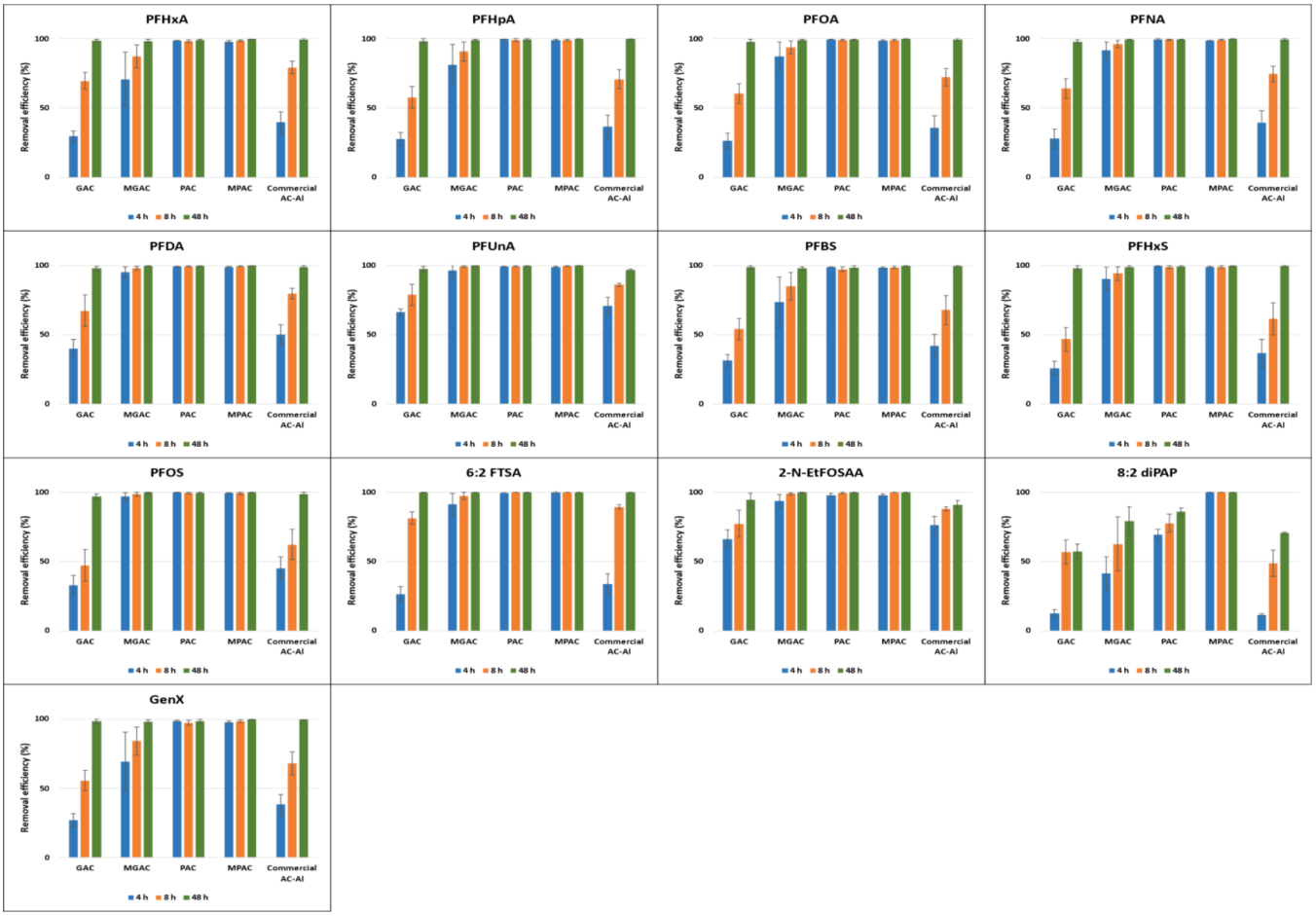

Figure 2. Adsorption of PFAS by unmodified and modified GAC and PAC and a commercial AC-Al-based sorbent at 4, 8, and 48 h. Initial PFAS concentration: 10 μg/L, and sorbent dose: 100 mg/L.

120 rpm for 48 h. The PFAS removal efficiency was calculated using eq 1 as follows:

$$\text{Removal efficiency}(\%) = \frac{C_i - C_t}{C_i} \times 100 \quad (1)$$

where C_i and C_t are the PFAS concentration that at initial and time (t), respectively.

Afterward, MPAC with the best adsorption performance (i.e., 90:10 PAC:FeOOH) was selected and tested against PAC, GAC, MGAC (90:10 GAC:FeOOH), and a commercial AC-aluminum (AC-Al)-based sorbent for the adsorption of 13 PFAS, each at 10 μg/L. These 13 PFAS included 6:2 FTSA and 2-N-EtFOSAA in addition to the 11 tested previously. For this test, subsamples were collected at 0, 4, 8, and 48 h and subjected to PFAS analysis.

The experimental details of the adsorption kinetics and isotherms are shown in Text S1, while the details of the sorbents' characterization and PFAS analysis are given in Texts S2 and S3, respectively.

3. RESULTS AND DISCUSSION

3.1. Modification of PAC for PFAS Adsorption. To enhance PFAS adsorption by a commercial PAC, the PAC was modified by incorporating different amounts of FeOOH or kaolin (Table S3). As shown in Figure 1, the main observations are (1) the modification of PAC by both FeOOH and kaolin did not lead to increased PFAS adsorption at the low concentration of 100 ng/L. This was true for all short and long-chain PFAS adsorption except for PFDA and PFUnA (see Table S1 for abbreviation definitions); (2) all modified PAC had higher removal of 8:2 diPAP than the pristine PAC. Especially, MPAC (90:10 of PAC: FeOOH) removed >80% of 8:2diPAP, while pristine PAC showed <25% removal of this precursor; (3) the loading of kaolin onto PAC/FeOOH did not improve the adsorption performance. On the contrary, the removal % was reduced, possibly due to blocking the active sites for PFAS adsorption; (4) among the different ratios of PAC, FeOOH, and kaolin tested, 90:10 of PAC:FeOOH (MPAC) showed the best performance for removal of a mixture of 11 PFAS, each at 100 ng/L.

3.2. PFAS Adsorption of MGAC and MPAC. To determine the adsorption equilibrium time of PFAS on GAC, PAC, MGAC, MPAC, and a commercial AC-Al sorbent, subsamples were collected at 0, 4, 8, and 48 h, as shown in Figure 2. It was observed that MPAC had the highest removal of all PFAS compared to MGAC, PAC, GAC, and the AC-Al-based commercial sorbent. Both PAC and MPAC achieved 100% removal of long- and short-chain PFAAs, 6:2 FTSA, GenX, and 2-N-EtFOSAA in 4 h. For 8:2 diPAP, however, PAC needed 48 h to reach 85% removal. The adsorption performance of the commercial AC-Al sorbent was below 50% at 1 h except for 2-N-EtFOSAA (ca. 75%) and gradually increased with time and reached 100% removal at 48 h for

https://doi.org/10.1021/acsestwater.3c00483
ACS EST Water 2023, 3, 3708−3715

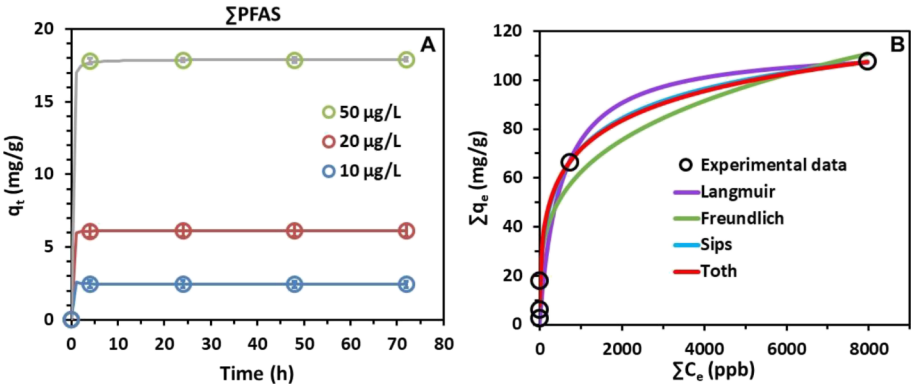

Figure 3. (A) Kinetics of PFAS adsorption at an initial concentration of 10, 20, or 50 μg/L for individual PFAS by MPAC and (B) adsorption isotherms of total PFAS by MPAC, fitted by the Langmuir, Freundlich, Sips, and Toth models.

Table 1. Parameters and Values Derived from Isotherm Models for PFAS Adsorption by MPAC

Langmuir		Freundlich		Sips		Toth	
parameter	value	parameter	value	parameter	value	parameter	value
R^2	0.9836	R^2	0.9734	R^2	0.9886	R^2	0.9892
K_L (L/μg)	1.92×10^{-3}	K_F (mg·L$^{1/m}$/(g·μg$^{1/m}$))	9.16	K_S (L/μg)	3.44×10^{-2}	K_T (L/μg)	0.20
q_m (mg/g)	114.13	m	3.60	q_m (mg/g)	153.56	q_m (mg/g)	234.43
				n	2.13	t	0.22

most PFAS. The exception was 8:2 diPAP, for which only 70% was removed at 48 h.

Reports on PFAS adsorption by modified GAC are very limited in the literature. In this study, removal of all tested PFAS, each at 10 μg/L by GAC increased with time from 4 to 48 h, with nearly 100% removal of PFAAs, GenX, 2-N-EtFOSAA, and 6:2 FTSA observed at 48 h. Compared to GAC, MGAC had a much faster adsorption rate for all PFAS. Among all of the targeted PFAS, 8:2 diPAP was an exception. Its removal by GAC and MGAC after 48 h was 58 and 80%, respectively. Given the outstanding performance of MPAC for removing all tested PFAS, this sorbent was studied further in terms of structure characterization, adsorption isotherms, kinetics, and removal mechanism, as shown below.

3.3. Kinetics and isotherm studies. The adsorption kinetics of the MPAC was investigated by using three kinetic models: pseudo-first-order (PFO), pseudo-second-order (PSO), and intra-particle diffusion (IPD) (see the Supporting Information). The adsorption data of total PFAS were fitted to these models, and the fitting correlations were assessed. The squared correlation coefficients (R^2) obtained from the linearized PFO and IPD models were 0.0001 and 0.436, respectively (Figure S1), indicating low fitting correlations. In contrast, the linearized PSO model exhibited excellent fitting correlations with an R^2 value of 0.998 (Figure S1), suggesting that the PSO model described the adsorption kinetics well. Consequently, PSO was employed to fit the kinetic data of the total PFAS (Figure 3A). The results indicated that a rapid adsorption of total PFAS occurred within the initial hours of contact time, demonstrating the fast kinetics of MPAC compared to the others in the literature, as shown in Table 2 ranging from 12 h to 10 days.

Four commonly used isotherm models, namely, Langmuir, Freundlich, Sips, and Toth, were employed to fit the experimental adsorption data (Figure 3B). The Langmuir isotherm accounts for the dynamic equilibrium of adsorption and desorption, while the Freundlich isotherm describes the adsorption process on heterogeneous surfaces. The Sips and Toth models combine elements of the Langmuir and Freundlich isotherms, with the primary objective of predicting adsorption behaviors in heterogeneous systems. The q_e and C_e values for total PFAS (ΣPFAS) were calculated and used to establish isotherm models because some individual PFAS in the aqueous phase were either near or below the limit of detection and similar physicochemical properties and adsorption mechanisms were possibly shared among the examined PFAS. The relationship between C_0 and mass of PFAS adsorbed by the MPAC can be found in Figure S2.

As shown in Figure 3B and summarized in Tables 1 and S4, the Langmuir model provided a good fit for the experimental adsorption data in the high-concentration range, while the Freundlich isotherm exhibited an excellent fit in the low-concentration range. The Sips and Toth isotherms satisfactorily described the entire range of data, indicating the successful application of the Sips isotherm in modeling the adsorption process. The Sips isotherm is known to address the limitations associated with an increasing adsorbate concentration in the Freundlich model. It essentially behaves like the Freundlich model at low adsorbate concentrations and predicts monolayer adsorption, similar to the Langmuir model at high adsorbate concentrations. Between the Sips and Toth isotherms, Toth had a better fit given R^2 of 0.9892, higher than 0.9886 of the Sips. The Toth model predicted a maximum adsorption capacity of 234.43 mg of PFAS/g of MPAC.

From Table 2, it was observed that the MPAC exhibited comparable maximum adsorption capacity with those reported. Different from other studies where only one or a few single PFAS at the mg/L level was targeted, the MPAC in this study had an excellent adsorption capacity for a PFAS mixture at the low end of μg/L levels that are environmentally relevant. It was also noted that during adsorption, with the increase of time, long-chain PFAS did not outcompete and led to desorption of the short-chain ones within the tested 48 h. Thus, the MPAC

https://doi.org/10.1021/acsestwater.3c00483
ACS EST Water 2023, 3, 3708−3715

Table 2. Adsorption Capacity Comparison of the Prepared MPAC in the Present Study with Similar Sorbents Reported in the Literature[a]

no.	sorbent	BET surface area (m^2/g)	dose (mg/L)	PFAS studied	C_0 (mg/L)	time point (h)	isotherm	sorption capacity (mg/g)
1	MPAC (this study)	493	100	PFHxA, PFHpA, PFOA, PFNA, PFDA, PFUnA, PFBS, PFHxS, PFOS, 6:2 FTSA, 2-N-EtFOSAA and GenX	0.01–0.5	4	Toth	234.43 (total PFAS)
2	magnetic (Fe_3O_4) modified PAC[26]	400	140	PFOA, PFHxS, PFBS and PFOS	PFOA: 21–298; PFHxS: 20–288; PFBS: 15–216; PFOS: 25–360	N/A	Langmuir: PFOA, PFHxS, PFBS; Freundlich: PFOS	PFOA: 373; PFHxS: 132; PFBS: 63; PFOS: 725
3	HCl modified GAC F4100[28]	899	10	PFHxS and PFOA	PFHxS: 1; PFOA: 1	10 days	N/A	PFHxS: 13.4; PFOA: 14.6
4	polyDADMAC-GAC[29]	536	200	PFBA and PFOA	PFBA: 1; PFOA: 1	96	Langmuir	PFBA: 165. 68; PFOA: 313.77
5	chitosan-GAC[30]	537	10	PFOA	10–200	72	Langmuir	298.1
6	PAC[31]	745	10	GenX	0.06–0.91 mmol	96	Langmuir	260.7
7	PAC[32]	812	N/A	PFOA and PFOS	20 to 250	12	Langmuir	PFOA: 219.4; PFOS: 520.1

[a]Note: N/A: not available; C_0 is the initial PFAS concentration (mg/L).

has a high potential for removing PFAS present as mixtures in various environmental matrices.

3.4. Physicochemical Characterization Studies.

3.4.1. FTIR and TGA. To reveal the functional groups of the PAC, MPAC, and PFAS-laden MPAC, Fourier transform infrared spectroscopy (FTIR) was performed as shown in Figure S3A. It was difficult to identify FTIR bands of functional groups associated with their structure. A few bands were identified as follows: the band at 3650 cm^{-1} due to the OH stretch demonstrates the evaporation of moisture.[33] FTIR spectra of PAC had the stretching vibration of COO−[34] and C−O bonds[35] at 1540 and 1100 cm^{-1}, respectively. Similar bands were also noticed in the FTIR spectra of MPAC. Next, the Fe−O bond of amorphous goethite is observed by the FTIR spectra of MPAC at 1394 cm^{-1}[36] confirming that Fe^{3+} is loaded with PAC. FTIR bands of C═O groups (1682 cm^{-1}) and the C═C bond of aromatic rings (1477 cm^{-1}) appeared in both PAC and MPAC.[37] The FTIR spectra of PFAS-laden MPAC had all the individual FTIR bands of both PAC and MPAC with slightly altered signals which denotes the interactions between the PFAS molecules and MPAC surface.[38]

The thermal characteristics of GAC, PAC, MGAC, and MPAC were investigated through thermogravimetric analysis (TGA) under a N_2 atmosphere from 45 to 1000 °C, as depicted in Figure S3B. The weight loss observed at temperatures below 120 °C for all sorbents was attributed to the evaporation of water molecules present in the pores of the sorbent; noticeably, MPAC had a higher weight loss (∼8%) at this stage. A significant reduction in weight of GAC and PAC was observed at 900 °C. For MGAC and MPAC, minor weight losses (<2%) were detected in the range of 350−400 and 650−700 °C, respectively. Overall, there was no significant thermally driven mass loss observed below 800 °C, suggesting that these sorbents can withstand high temperatures, which is a favorable indicator for their stability in applications where thermal stress may be a concern. Aside from thermal stress, other stress factors, such as mechanical stress, exposure to other non-PFAS chemicals, repeated cycles of adsorption−desorption will need to be investigated to understand the sorbents' stability in real-world applications.

3.4.2. SEM, EDS, and BET. Scanning electron microscopy (SEM) images presented in Figure S4 depict the morphologies of GAC, MGAC, PAC, MPAC, and PFAS-laden MGAC and MPAC at 200 nm. Both GAC and PAC displayed coarse surfaces, as shown in Figure S4A,D. Subsequent to the modification process, a uniform surface exhibiting increased macroporosity was observed in MGAC and MPAC. These data suggested that the iron deposition exhibited a strong adherence to the surfaces of both GAC and PAC (Figure S4B,E). The change in the morphology of SEM images of PFAS-laden MGAC and MPAC (Figure S4C,F) is due to the surface coverage of PFAS molecules via adsorption.

Energy-dispersive spectrometry (EDS) spectra showing elemental composition (Figure S5) provided further evidence of increased atomic % for Fe on the surface of MGAC (8.29%) and MPAC (10.91%) in comparison to their pristine counterparts. The presence of calcium, magnesium, and aluminum in all four sorbents agreed with prior research findings.[39] The presence of the predominant fluorine (F) peak in the EDS spectra of the PFAS-laden both MGAC and MPAC with atomic % values of 3.07 and 7.30%, respectively, confirms that PFAS was adsorbed to their surfaces.

https://doi.org/10.1021/acsestwater.3c00483
ACS EST Water 2023, 3, 3708−3715

The total surface area of GAC, MGAC, PAC, and MPAC was calculated as 972, 940, 433, and 493 m^2/g, respectively, using the Brunauer−Emmett−Teller (BET) isotherm. Among these sorbents, GAC had a higher surface area than PAC, which is similar to previous findings.[40,41] The BET surface area of the MGAC experienced a reduction of approximately 3.3% as a result of the infusion of iron particles onto its surface, which is in line with a reported study.[42] The BET surface area of the MPAC, however, exhibited an increase of approximately 13%, possibly due to the microporous surface of the PAC/MPAC.[43,44] The microporous feature was supported by the high ratio of micropore area to total surface area (>63%). One of the advantages of the fine powder nature of PAC/MPAC is easy for mass transfer with a short diffusion path, allowing adsorbed PFAS molecules to reach available internal pores fast.[45]

3.5. Adsorption Mechanisms. The plausible removal mechanism of PFAS onto MPAC is mainly hydrophobic and electrostatic interactions, as shown in Figure 4. The hydrophobic interactions strongly depend on the C−F tail of the PFAS chain and hydrophobic C−C groups of the MPAC network. The abundant C−C groups of MPAC are attracted by the electronegative fluorine (C−F) of PFAS (especially long and relatively hydrophobic PFAS) via hydrophobic interactions.[26] The electrostatic interactions take place between the PFAS headgroup functionality and the surface charge of the sorbent. Specific to MPAC, the Fe^{3+} ions on its surface are able to attract anionic functional groups such as COO^- and SO_3^- of PFAS.[46] Thus, theoretically, the adsorption between short-chain PFCAs and PFSAs and MPAC is predominantly controlled by electrostatic interactions. Regarding the impacts on desorption, hydrophobic interaction tends to be stronger and more stable, which can make desorption more challenging. Desorbing PFAS molecules that are strongly bound via hydrophobic interactions may require more energy and/or specific desorbing agents.[47,48] In contrast, the electrostatic interaction is relatively weaker. PFAS molecules adsorbed through electrostatic attractions may be more easily desorbed under the appropriate conditions.

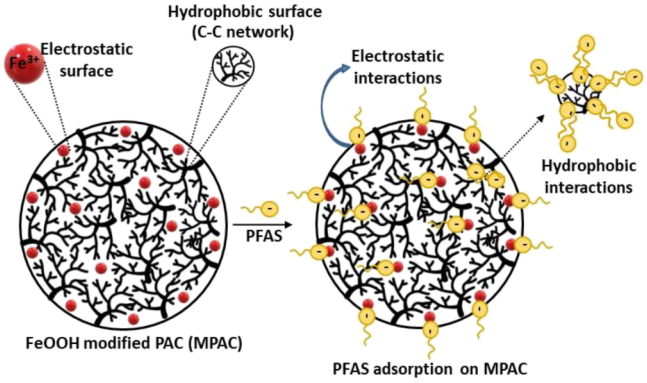

Figure 4. Plausible mechanisms for PFAS adsorption on MPAC.

From the literature, the Langmuir isotherm was observed to be significantly influenced by electrostatic interactions,[49] while the Freundlich isotherm exhibited a strong correlation with hydrophobic interactions.[50] Our adsorption data matched the Toth isotherm better at high concentrations than at low concentrations, lending credence to the idea that electrostatic interactions predominated at high concentrations, while hydrophobic attractions took over at low concentrations. The model exhibits conformity with the low concentration limit of the Langmuir equation model and converges toward the Freundlich model at a high concentration.[51,52] The other weak interactions such as hydrogen bonding, van der Waals, and pore filling are also possible on the MPAC surface due to the available −COOH/−OH functional group and MPAC's porous nature.[17,53] However, additional empirical and theoretical analyses would be required to authenticate the suggested PFAS adsorption/desorption mechanism. The implementation of a verified mechanism would prove advantageous in the development of improved sorbents for the purpose of PFAS removal through an iterative cycle of redesign and retest.

4. CONCLUSIONS

While GAC and PAC are well-known and widely used sorbents for PFAS removal, MGAC and MPAC reported in this study had much better performance for the adsorption of a mixture of PFAS at environmentally relevant concentrations. The MPAC in particular had 100% removal of 8:2 diPAP, demonstrating its potential use in removing PFAS precursors that are widely present in the environment. This study thus provided two new sorbents, MGAC and MPAC, that can possibly replace GAC and PAC for removing PFAS in real water contaminated by these emerging pollutants.

■ ASSOCIATED CONTENT

Supporting Information

The Supporting Information is available free of charge at https://pubs.acs.org/doi/10.1021/acsestwater.3c00483.

Physiochemical properties of PFAS; details of chemicals/reagents; experimental details of adsorption, isotherms, and kinetics; PFAS analysis; analysis of adsorption data, isotherm, and kinetics; and sorbent characterization by FTIR, TGA, SEM, and EDS (PDF)

■ AUTHOR INFORMATION

Corresponding Author

Weilan Zhang − *Department of Environmental and Sustainable Engineering, University at Albany, State University of New York, Albany, New York 12222, United States;* orcid.org/0000-0003-3148-1751; Email: wzhang4@albany.edu

Authors

Aswin Kumar Ilango − *Department of Environmental and Sustainable Engineering, University at Albany, State University of New York, Albany, New York 12222, United States;* orcid.org/0000-0002-0679-8880

Tao Jiang − *Department of Environmental and Sustainable Engineering, University at Albany, State University of New York, Albany, New York 12222, United States;* orcid.org/0000-0003-1582-9885

Md. Nahid Pervez − *Department of Environmental and Sustainable Engineering, University at Albany, State University of New York, Albany, New York 12222, United States;* orcid.org/0000-0001-6187-5351

Jeremy I. Feldblyum − *Department of Chemistry, University at Albany, State University of New York, Albany, New York 12222, United States;* orcid.org/0000-0001-6667-9587

https://doi.org/10.1021/acsestwater.3c00483
ACS EST Water 2023, 3, 3708−3715

Haralabos Efstathiadis − *Department of Nanoscale Science and Engineering, University at Albany, State University of New York, Albany, New York 12222, United States*

Yanna Liang − *Department of Environmental and Sustainable Engineering, University at Albany, State University of New York, Albany, New York 12222, United States;* orcid.org/0000-0003-1720-1039

Complete contact information is available at: https://pubs.acs.org/10.1021/acsestwater.3c00483

Author Contributions

‖A.K.I. and T.J. contributed equally to this work. CRediT: **Aswin Kumar Ilango** conceptualization, data curation, formal analysis, investigation, methodology, software, validation, visualization, writing-original draft, writing-review & editing; **Tao Jiang** conceptualization, data curation, formal analysis, investigation, methodology, software, validation, visualization, writing-original draft, writing-review & editing; **Weilan Zhang** conceptualization, data curation, formal analysis, investigation, methodology, validation, visualization, writing-review & editing; **Md. Nahid Pervez** formal analysis, writing-review & editing; **Jeremy I. Feldblyum** resources, writing-review & editing; **Haralabos Efstathiadis** resources, writing-review & editing; **Yanna Liang** funding acquisition, project administration, resources, supervision, validation, visualization, writing-review & editing.

Notes

The authors declare no competing financial interest.

■ ACKNOWLEDGMENTS

The authors acknowledge financial support from the U.S. National Science Foundation under award number CBET 2225596. The authors are also grateful to Kevin Shah from SUNY Polytechnic Institute for his assistance with SEM-EDS measurements and to Audrey Crom from SUNY Albany for BET analyses. Support for thermogravimetry experiments was provided by National Science Foundation grant CHE-1919810.

■ REFERENCES

(1) Nakayama, S. F.; Yoshikane, M.; Onoda, Y.; Nishihama, Y.; Iwai-shimada, M.; Takagi, M.; Kobayashi, Y.; Isobe, T. Worldwide trends in tracing poly-and perfluoroalkyl substances (PFAS) in the environment. *TrAC, Trends Anal. Chem.* **2019**, *121*, 115410.

(2) Buck, R. C.; Franklin, J.; Berger, U.; Conder, J. M.; Cousins, I. T.; De voogt, P.; Jensen, A. A.; Kannan, K.; Mabury, S. A.; Van leeuwen, S. P. Perfluoroalkyl and polyfluoroalkyl substances in the environment: terminology, classification, and origins. *Integr. Environ. Assess. Manage.* **2011**, *7* (4), 513−541.

(3) Vickers, N. J. Animal communication: when i'm calling you, will you answer too? *Curr. Biol.* **2017**, *27* (14), R713−R715.

(4) Jiang, T.; Geisler, M.; Zhang, W.; Liang, Y. Fluoroalkylether compounds affect microbial community structures and abundance of nitrogen cycle-related genes in soil-microbe-plant systems. *Ecotoxicol. Environ. Safety* **2021**, *228*, No. 113033.

(5) Jiang, T.; Zhang, W.; Liang, Y. Uptake of individual and mixed per-and polyfluoroalkyl substances (PFAS) by soybean and their effects on functional genes related to nitrification, denitrification, and nitrogen fixation. *Sci. Total Environ.* **2022**, *838*, No. 156640.

(6) U.S.EPA. *Drinking Water Health Advisories for PFOA and PFOS.* https://www.epa.gov/sdwa/drinking-water-health-advisories-pfoa-and-pfos (accessed August 2023).

(7) Stratton, G. R.; Dai, F.; Bellona, C. L.; Holsen, T. M.; Dickenson, E. R.; Mededovic thagard, S. Plasma-based water treatment: efficient transformation of perfluoroalkyl substances in prepared solutions and contaminated groundwater. *Environ. Sci. Technol.* **2017**, *51* (3), 1643−1648.

(8) Ross, I.; Mcdonough, J.; Miles, J.; Storch, P.; Thelakkat kochunarayanan, P.; Kalve, E.; Hurst, J.; S. dasgupta, S.; Burdick, J. A review of emerging technologies for remediation of PFASs. *Remediat. J.* **2018**, *28* (2), 101−126.

(9) Arvaniti, O. S.; Stasinakis, A. S. Review on the occurrence, fate and removal of perfluorinated compounds during wastewater treatment. *Sci. Total Environ.* **2015**, *524*, 81−92.

(10) Finnegan, C.; Ryan, D.; Enright, A.-M.; Garcia-cabellos, G. A review of strategies for the detection and remediation of organotin pollution. *Crit. Rev. Environ. Sci. Technol.* **2018**, *48* (1), 77−118.

(11) Appleman, T. D.; Higgins, C. P.; Quiñones, O.; Vanderford, B. J.; Kolstad, C.; Zeigler-holady, J. C.; Dickenson, E. R. Treatment of poly-and perfluoroalkyl substances in US full-scale water treatment systems. *Water Res.* **2014**, *51*, 246−255.

(12) Rahman, M. F.; Peldszus, S.; Anderson, W. B. Behaviour and fate of perfluoroalkyl and polyfluoroalkyl substances (PFASs) in drinking water treatment: A review. *Water Res.* **2014**, *50*, 318−340.

(13) Liu, L.; Li, Y.; Coelhan, M.; Chan, H. M.; Ma, W.; Liu, L. Relative developmental toxicity of short-chain chlorinated paraffins in Zebrafish (Danio rerio) embryos. *Environ. Pollut.* **2016**, *219*, 1122−1130.

(14) Carter, K. E.; Farrell, J. Removal of perfluorooctane and perfluorobutane sulfonate from water via carbon adsorption and ion exchange. *Sep. Sci. Technol.* **2010**, *45* (6), 762−767.

(15) Jiang, T.; Zhang, W.; Ilango, A. K.; Feldblyum, J. I.; Wei, Z.; Efstathiadis, H.; Yigit, M. V.; Liang, Y. Surfactant-Modified Clay for Adsorption of Mixtures of Per-and Polyfluoroalkyl Substances (PFAS) in Aqueous Solutions. *ACS Appl. Eng. Mater.* **2023**, *1* (1), 394−407.

(16) Mccleaf, P.; Englund, S.; Östlund, A.; Lindegren, K.; Wiberg, K.; Ahrens, L. Removal efficiency of multiple poly-and perfluoroalkyl substances (PFASs) in drinking water using granular activated carbon (GAC) and anion exchange (AE) column tests. *Water Res.* **2017**, *120*, 77−87.

(17) Chen, W.; Zhang, X.; Mamadiev, M.; Wang, Z. Sorption of perfluorooctane sulfonate and perfluorooctanoate on polyacrylonitrile fiber-derived activated carbon fibers: in comparison with activated carbon. *RSC Adv.* **2017**, *7* (2), 927−938.

(18) Boyer, T. H.; Fang, Y.; Ellis, A.; Dietz, R.; Choi, Y. J.; Schaefer, C. E.; Higgins, C. P.; Strathmann, T. J. Anion exchange resin removal of per-and polyfluoroalkyl substances (PFAS) from impacted water: A critical review. *Water Res.* **2021**, *200*, No. 117244.

(19) Ilango, A. K.; Jiang, T.; Zhang, W.; Feldblyum, J. I.; Efstathiadis, H.; Liang, Y. Surface-modified biopolymers for removing mixtures of per- and polyfluoroalkyl substances from water: Screening and removal mechanisms. *Environ. Pollut.* **2023**, *331*, No. 121865.

(20) Saha, D.; Khan, S.; Van bramer, S. E. Can porous carbons be a remedy for PFAS pollution in water? A perspective. *J. Environ. Chem. Eng.* **2021**, *9* (6), No. 106665.

(21) Xiao, X.; Ulrich, B. A.; Chen, B.; Higgins, C. P. Sorption of poly-and perfluoroalkyl substances (PFASs) relevant to aqueous film-forming foam (AFFF)-impacted groundwater by biochars and activated carbon. *Environ. Sci. Technol.* **2017**, *51* (11), 6342−6351.

(22) Dudley, L.-A. *Removal of Perfluorinated Compounds by Powdered Activated Carbon, Superfine Powder Activated Carbon, and Anion Exchange Resin*. Master Thesis, North Carolina State University: Raleigh, NC, 2012.

(23) Oladipo, A. A.; Gazi, M. Enhanced removal of crystal violet by low cost alginate/acid activated bentonite composite beads: optimization and modelling using non-linear regression technique. *J. Water Process Eng.* **2014**, *2*, 43−52.

(24) Li, Q.; Li, R.; Ma, X.; Sarkar, B.; Sun, X.; Bolan, N. Comparative removal of As(V) and Sb(V) from aqueous solution by sulfide-modified α-FeOOH. *Environ. Pollut.* **2020**, *267*, No. 115658.

(25) Lee, S.; Lee, T.; Kim, D. Adsorption of hydrogen sulfide from gas streams using the amorphous composite of α-FeOOH and

activated carbon powder. *Ind. Eng. Chem. Res.* **2017**, *56* (11), 3116−3122.
(26) Meng, P.; Fang, X.; Maimaiti, A.; Yu, G.; Deng, S. Efficient removal of perfluorinated compounds from water using a regenerable magnetic activated carbon. *Chemosphere* **2019**, *224*, 187−194.
(27) Tan, H.-M.; Pan, C.-G.; Yin, C.; Yu, K. Toward systematic understanding of adsorptive removal of legacy and emerging per-and polyfluoroalkyl substances (PFASs) by various activated carbons (ACs). *Environ. Res.* **2023**, *233*, No. 116495.
(28) Siriwardena, D. P.; Crimi, M.; Holsen, T. M.; Bellona, C.; Divine, C.; Dickenson, E. Changes in adsorption behavior of perfluorooctanoic acid and perfluorohexanesulfonic acid through chemically-facilitated surface modification of granular activated carbon. *Environ. Eng. Sci.* **2019**, *36* (4), 453−465.
(29) Ramos, P.; Singh kalra, S.; Johnson, N. W.; Khor, C. M.; Borthakur, A.; Cranmer, B.; Dooley, G.; Mohanty, S. K.; Jassby, D.; Blotevogel, J.; Mahendra, S. Enhanced removal of per- and polyfluoroalkyl substances in complex matrices by polyDADMAC-coated regenerable granular activated carbon. *Environ. Pollut.* **2022**, *294*, No. 118603.
(30) Liu, W.; Lin, T.; Zhang, X.; Jiang, F.; Yan, X.; Chen, H. Adsorption of perfluoroalkyl acids on granular activated carbon supported chitosan: Role of nanobubbles. *Chemosphere* **2022**, *309*, No. 136733.
(31) Wang, W.; Maimaiti, A.; Shi, H.; Wu, R.; Wang, R.; Li, Z.; Qi, D.; Yu, G.; Deng, S. Adsorption behavior and mechanism of emerging perfluoro-2-propoxypropanoic acid (GenX) on activated carbons and resins. *Chem. Eng. J.* **2019**, *364*, 132−138.
(32) Yu, Q.; Zhang, R.; Deng, S.; Huang, J.; Yu, G. Sorption of perfluorooctane sulfonate and perfluorooctanoate on activated carbons and resin: Kinetic and isotherm study. *Water Res.* **2009**, *43* (4), 1150−1158.
(33) Deligeer, W.; Gao, Y.; Asuha, S. Adsorption of methyl orange on mesoporous γ-Fe2O3/SiO2 nanocomposites. *Appl. Surf. Sci.* **2011**, *257* (8), 3524−3528.
(34) Wahab, M. A.; Jellali, S.; Jedidi, N. Ammonium biosorption onto sawdust: FTIR analysis, kinetics and adsorption isotherms modeling. *Bioresour. Technol.* **2010**, *101* (14), 5070−5075.
(35) Hamid, Y.; Liu, L.; Usman, M.; Naidu, R.; Haris, M.; Lin, Q.; Ulhassan, Z.; Hussain, M. I.; Yang, X. Functionalized biochars: Synthesis, characterization, and applications for removing trace elements from water. *J. Hazard. Mater.* **2022**, *437*, No. 129337.
(36) Jiao, F.; Yu, J.; Song, H.; Jiang, X.; Yang, H.; Shi, S.; Chen, X.; Yang, W. Excellent adsorption of Acid Flavine 2G by MgAl-mixed metal oxides with magnetic iron oxide. *Appl. Clay Sci.* **2014**, *101*, 30−37.
(37) Njoku, V. O.; Hameed, B. H. Preparation and characterization of activated carbon from corncob by chemical activation with H3PO4 for 2,4-dichlorophenoxyacetic acid adsorption. *Chem. Eng. J.* **2011**, *173* (2), 391−399.
(38) Pourrezaei, P.; Alpatova, A.; Chelme-ayala, P.; Perez-estrada, L. A.; Jensen-fontaine, M.; Le, X. C.; Gamal el-din, M. Impact of petroleum coke characteristics on the adsorption of the organic fractions from oil sands process-affected water. *Int. J. Environ. Sci. Technol.* **2014**, *11* (7), 2037−2050.
(39) Barjasteh-askari, F.; Davoudi, M.; Dolatabadi, M.; Ahmadzadeh, S. Iron-modified activated carbon derived from agro-waste for enhanced dye removal from aqueous solutions. *Heliyon* **2021**, *7* (6), No. e07191.
(40) Tao, X.; Xiaoqin, L. Peanut shell activated carbon: characterization, surface modification and adsorption of Pb2+ from aqueous solution. *Chinese J. Chem. Eng.* **2008**, *16* (3), 401−406.
(41) Kumar, A.; Prasad, B.; Mishra, I. Adsorptive removal of acrylonitrile by commercial grade activated carbon: kinetics, equilibrium and thermodynamics. *J. Hazard. Mater.* **2008**, *152* (2), 589−600.
(42) Barua, S.; Zakaria, B. S.; Lin, L.; Dhar, B. R. Magnetite doped granular activated carbon as an additive for high-performance anaerobic digestion. *Mater. Sci. Energy Technol.* **2019**, *2* (3), 377−384.
(43) El-merraoui, M.; Aoshima, M.; Kaneko, K. Micropore Size Distribution of Activated Carbon Fiber Using the Density Functional Theory and Other Methods. *Langmuir* **2000**, *16* (9), 4300−4304.
(44) Serafin, J.; Narkiewicz, U.; Morawski, A. W.; Wróbel, R. J.; Michalkiewicz, B. Highly microporous activated carbons from biomass for CO2 capture and effective micropores at different conditions. *J. CO2 Util.* **2017**, *18*, 73−79.
(45) Pramanik, B. K.; Pramanik, S. K.; Suja, F. A comparative study of coagulation, granular-and powdered-activated carbon for the removal of perfluorooctane sulfonate and perfluorooctanoate in drinking water treatment. *Environ. Technol.* **2015**, *36* (20), 2610−2617.
(46) Zhao, C.; Xu, Y.; Xiao, F.; Ma, J.; Zou, Y.; Tang, W. Perfluorooctane sulfonate removal by metal-organic frameworks (MOFs): Insights into the effect and mechanism of metal nodes and organic ligands. *Chem. Eng. J.* **2021**, *406*, No. 126852.
(47) Liu, K.; Zhang, S.; Hu, X.; Zhang, K.; Roy, A.; Yu, G. Understanding the Adsorption of PFOA on MIL-101(Cr)-Based Anionic-Exchange Metal−Organic Frameworks: Comparing DFT Calculations with Aqueous Sorption Experiments. *Environ. Sci. Technol.* **2015**, *49* (14), 8657−8665.
(48) Ateia, M.; Alsbaiee, A.; Karanfil, T.; Dichtel, W. Efficient PFAS removal by amine-functionalized sorbents: critical review of the current literature. *Environ. Sci. Technol. Lett.* **2019**, *6* (12), 688−695.
(49) Hartvig, R. A.; Van de weert, M.; Østergaard, J.; Jorgensen, L.; Jensen, H. Protein Adsorption at Charged Surfaces: The Role of Electrostatic Interactions and Interfacial Charge Regulation. *Langmuir* **2011**, *27* (6), 2634−2643.
(50) Das, P.; Arias, E. V. A.; Kambala, V.; Mallavarapu, M.; Naidu, R. Remediation of Perfluorooctane Sulfonate in Contaminated Soils by Modified Clay Adsorbent—a Risk-Based Approach. *Water, Air, Soil Pollut.* **2013**, *224* (12), 1714.
(51) Dhaouadi, H.; M'henni, F. Vat dye sorption onto crude dehydrated sewage sludge. *J. Hazard. Mater.* **2009**, *164* (2−3), 448−458.
(52) Yu, J.; Hu, J.; Tanaka, S.; Fujii, S. Perfluorooctane sulfonate (PFOS) and perfluorooctanoic acid (PFOA) in sewage treatment plants. *Water Res.* **2009**, *43* (9), 2399−2408.
(53) Appleman, T. D.; Dickenson, E. R.; Bellona, C.; Higgins, C. P. Nanofiltration and granular activated carbon treatment of perfluoroalkyl acids. *J. Hazard. Mater.* **2013**, *260*, 740−746.

https://doi.org/10.1021/acsestwater.3c00483
ACS EST Water 2023, 3, 3708−3715